Visnyk NTUU KPI Seriia – Radiotekhnika Radioaparatobuduvannia, 2016, Iss. 67, pp. 50–57

Peculiarities of signal formation of the autodyne short-range radar with linear frequency modulation

Noskov, V. Y.[1], *Ignatkov, K. A.*[1], *Chupahin, A. P.*[1], *Vasiliev, A. V.*[2], *Ermak, G. P.*[2], *Smolskiy, S. M.*[3]

[1]Ural Federal University, Ekaterinburg, Russia
[2]O.Ya. Usikov Institute for Radiophysics and Electronics, Kharkiv, Ukraine
[3]National Research University "Moscow Power Engineering Institute", Moskow, Russia

E-mail: *noskov@oko-ek.ru*

Research results of signal formation peculiarities in autodyne short-range radars with linear frequency modulation by non-symmetric saw-tooth law are presented. Calculation expressions for autodyne signals are obtained in the general case of arbitrary delay time of reflected emission. Temporal and spectral diagrams of autodyne signals are defined in the cases when its period duration is much more than the delay time of reflected emission, as well as for cases when this inequality is not satisfied. Experimental investigations are performed using the autodyne oscillator on the Gunn diode of 8mm-range, which is electronically controlled in frequency by the varicap.

Key words: autodyne; autodyne signal; autodyne response; short-range radar; frequency modulation; Gunn-diode oscillator

Introduction

Autodyne short range radars with frequency modulation (FM ASRR) have found wide application as guard sensors, anti-collision sensors for transport vehicles, measuring devices for car motion in hump yards, detectors of point-work occupation and railway crossings and many others [1–5] due to construction simplicity and low cost of the transceiver device. Operation principle of these devices is based on the so-called "autodyne effect", which consists in oscillator parameter variations under influence of reflected emission [5]. These variations registration in the form of autodyne signals and their further processing provide a possibility to obtain information about reflecting object and its relative motion parameters.

A large number of publications is devoted to peculiarities of FM ASRR autodyne signal formation, in which different mathematical models and impact function representations for proper reflected emission are used. In earlier publications, which were mainly issued in the period of autodyne theory coming into being, the impact function was represented by variable load, which varies with a frequency of the signal formed [6]. In later publications, this function was described by the equivalent current (or voltage) source having the relative frequency offset caused by emission FM and by reflected radio-signal delay [5, 7–9]. Within the limits of described approaches, the oscillation frequency and amplitude are changing with the differential frequency and the output signals become harmonic as a result of these variation detection.

In publications of the recent time, the presence of anharmonic distortions [10, 11] at investigation of FM ASRR signal in the millimeter wavelength range. The phase delay of reflected emission was assumed as a basis of the model, which takes into consideration this phenomenon. At that, it was shown that signal distortions are caused by autodyne frequency variations, which cause nonlinearity of the reflected emission phase incursion. Nevertheless, solution of equations with retarded argument in known publications was obtained for the first approximation only, which is valid under condition, when the delay time τ of reflected emission in much less than the period T_a of formed autodyne signal. In the actual conditions, at large values of frequency deviations and the high FM operation speed, which is typical for millimeter-wave range, this inequality may be violated[1]. For such conditions of FM ASRR functioning, peculiarities of autodyne response formation did not consider in known publication.

To develop the promising FM ASRRs and its reasonable applications, it is undoubtedly necessary to have a knowledge about signal properties under mentioned conditions. Therefore, the goal of this paper is obtaining the general solution of the system of retarded equations for the single-circuit autodyne FM oscillator. Then, on the base of this solution, we are going to

[1]For example, in 8mm-range, in typical situation of 500 MHz frequency deviation [4], the frequency modulation by non-symmetric saw-tooth law equaled to 10 kHz and the distance to the object 75 m, the delay time τ is $0.5 \cdot 10^{-6}$ sec, and the autodyne signal period T_a is equal to $0.4 \cdot 10^{-6}$ sec.

examine peculiarities of autodyne response formation at different FM parameters and distances to the radar object for the non-symmetric saw-tooth FM law. Partially, this task were discussed in reports [12–14].

1 Initial expressions for signal analysis

A system of differential equations linearized in the vicinity of steady-state mode for small relative variations of the oscillation amplitude a and frequency χ for single-circuit oscillator, which is under impact of the proper reflected (from the radar object) emission, has a view [12, 15]:

$$(Q_L/\omega_{cav})(da/dt) + \alpha a + \varepsilon\chi = \Gamma(t,\tau)\eta\cos\delta(t,\tau), \quad (1)$$

$$\beta a + Q_L\chi = -\Gamma(t,\tau)\eta\sin\delta(t,\tau), \quad (2)$$

where Q_L, ω_{cav} are the loaded Q-factor and the cavity natural frequency, relatively; α, ε, and β are dimensionless parameters defining the oscillator increment slope, non-isodromity and non-isochronity, relatively; $\eta = Q_L/Q_{ex}$, Q_{ex} is an efficiency and the external Q-factor of the oscillating system; $\Gamma(t,\tau) = \Gamma_0[A(t,\tau)/A(t)]$, $\delta(t,\tau) = \Psi(t) - \Psi(t,\tau)$ are the modulus and the phase of the instantaneous reflection factor reduced to the oscillator output; Γ_0 is the emission damping factor in amplitude at its propagation to the object and back; $A(t)$, $A(t,\tau)$, and $\Psi(t)$, $\Psi(t,\tau)$ are oscillator amplitudes and phases in the current moment t and from the system pre-history $(t-\tau)$; $\tau = 2l/c$, where l is a distance to the reflecting object; c is the speed of emission propagation.

At FM by means of the bias voltage variations across the varicap, both frequency and "parasitic" amplitude modulation (PAM) occur:

$$\omega(t) = \omega_0 + \Delta\omega_{FM}(t) = \omega_0[1 + m_{FM}f_{mod}(t)], \quad (3)$$

$$A(t) = A_0[1 + a_{AM}(t)] = A_0[1 + a_{AM}f_{mod}(t)], \quad (4)$$

where $m_{FM} = \Delta\omega_{FM}/\omega_0$ and $m_{AM} = \Delta A_{AM}/A_0$ are coefficients of frequency (FM) and amplitude (AM) modulation, relatively; $\Delta\omega_{FM}$, ΔA_{AM} are maximal deviations of oscillation amplitude and frequency from the steady-state values A_0 and ω_0 due to oscillation modulation; $f_{mod}(t)$ is the normalized modulating function having the Ω_{mod} frequency. The quasi-static solutions of the first approximation [16] of the equation system (1), (2) with account (3), (4) for relative variations of the amplitude $a(t,\tau)$ and absolute frequency variations $\omega(t,\tau)$ of FM ASRR have a view:

$$a(t,\tau) = m_{AM}f_{mod}(t) + \Gamma(t,\tau)K_a\cos[\delta(t,\tau) - \psi], \quad (5)$$

$$\omega(t,\tau) = \omega_0\{1 + m_{AM}f_{mod}(t) - \Gamma(t,\tau)L_a \sin[\delta(t,\tau) + \theta]\}, \quad (6)$$

where K_a, L_a are coefficient of autodyne amplification and the frequency deviation; $\Psi = \arctan(\rho)$, $\theta = \arctan(\gamma)$ are angles of phase shift; $\rho = \varepsilon/Q_L$, $\gamma = \beta/\alpha$ are coefficients of oscillator non-isodromity and non-isochronity, relatively.

To obtain expressions describing the autodyne response in the general case of arbitrary ratio of reflected emission delay time τ and Ta period, we use the known approach to analysis of systems with delay, which is developed for the case of usual (without FM) autodyne signal description in [15]. Its sense consists in expansion of functions $A(t,\tau)$ and $\Psi(t,\tau)$ of retarded impact into Taylor series over the small parameter — ratio of delay time τ and the current time t. At that, we assume that functions (5), (6) have no breaks over all time interval for autodyne response formation. In addition, here we exclude from consideration the transients in reverse zones of the modulating functions taking into account fulfillment of the strong inequality $\tau << 2\pi/\Omega_{mod}$. Then, taking above-mentioned into consideration, expressions for $\Im(t,\tau)$ and $\delta(t,\tau)$ in (5), (6), as functions of normalized (dimensionless) delay times $\tau_n = \omega_0\tau/2\pi$ and the modulating function $t_n = \Omega_{mod}t/2\pi$, have the view:

$$\Gamma(t_n,\tau_n) = \Gamma_0\left(1 + 2\pi r_n\Gamma_0K_a\cdot \cdot\sum_{m=0}^{M}(-1)^m X_m(r_n)\sin[\delta(t_n,\tau_n) - \psi + \Theta_m(r_n)]\right) \quad (7)$$

$$\delta(t_n,\tau_n) = 2\pi\tau_n + \pi B_{FM}f_{mod}(t_n) - - C_{FB}\sum_{m=0}^{M}(-1)^m X_m(r_n)\sin[\delta(t_n,\tau_n) + \theta + \Theta_m(r_n)] \quad (8)$$

where $r_n = \tau/T_a$ is the parameter of normalized (with the respect to the autodyne signal period T_a) distance to reflecting object; $B_{FM} = \Delta F_{FM}\tau$ is the parameter of "FM base" defining the number of signal periods being stacked over the modulating function period at fixed reflecting object, when τ_n is fixed; $\Delta F_{FM} = \Delta\omega_{FM}/2\pi$ is the frequency deviation expressed in Hz; C_{FB} is the feedback parameter of the autodyne system; $X_m(r_n)$, $\Theta_m(r_n)$ are amplitude values and phase shifts of m-th terms $(m = 0, 1, \ldots, M)$ of series in equations (7) and (8):

$$X_m(r_n) = \frac{(2\pi r_n)^{2m}\sqrt{4(m+1)^2 + (2\pi r_n)^2}}{2(m+1)(2m+1)!}, \qquad \Theta_m(r_n) = -\arctan\frac{\pi r_n}{(m+1)} \quad (9)$$

Autodyne variations of oscillation amplitude Γ_0K_a are usually very small: $\Gamma_0K_a << 1$. Therefore, we can neglect by the second term in large parenthesis

of (7). Such an approximation in the autodyne system mathematical model supposes an account the phase delay only of the reflected emission. At that, we note that known solutions for the autodyne response following from (7) — (9), are obtained in the first approximations assuming $m = 0$. Account of series terms of higher order in these expressions, as it will shown later, allows taking into consideration also the dynamics of phase variation $\delta(t_n, \tau_n)$ at any ratio on delay time τ of reflected emission and the autodyne signal period T_a.

In this connection, the further analysis of the autodyne response will be examined without first terms in (5), (6) for $\Gamma(t, \tau) = \Gamma_0$. Then, expressions for normalized maximal values of variations of amplitude and frequency in the form of the amplitude (AAC) $a_n(t_n, \tau_n)$ and frequency AFA $\chi_n(t_n, \tau_n)$ characteristics[2] of the autodyne, have the vews:

$$a_n(t_n, \tau_n) = a(t_n, \tau_n)/\Gamma_0 K_a = \cos[\delta(t_n, \tau_n) - \psi], \quad (10)$$

$$\chi_n(t_n, \tau_n) = \chi(t_n, \tau_n)/\Gamma_0 L_a = -\sin[\delta(t_n, \tau_n) + \theta]. \quad (11)$$

Solution of the transcendent equation (8) under condition of its smoothness when $C_{FB} < 1$, can be obtained by the successive approximation method. This solution in the form of the autodyne phase characteristic (APC) $\delta(t_n, \tau_n)$ has a view:

$$\begin{aligned}\delta(t_n, \tau_n) &= \delta(t_n, \tau_n)_{(0)} - \\ &- C_{FB} \sum_{m=0}^{M} (-1)^m X_m(r_m) \sin[\delta(t_n, \tau_n)_{(1)} + \theta + \Theta_m(r_n) - \\ &- C_{FB} \sum_{m=0}^{M} (-1)^m X_m(r_n) \sin[\delta(t_n, \tau_n)_{(2)} + \theta + \Theta_m(r_n) - \dots \\ &- C_{FB} \sum_{m=0}^{M} (-1)^m X_m(r_n) \sin[\delta(t_n, \tau_n)_{(k)} + \theta + \Theta_m(r_n)] \dots \\ &\dots]] \quad (12)\end{aligned}$$

where indices in parenthesis near terms $\delta(t_n, \tau_n)$ denote the approximation order; $\delta(t_n, \tau_n)_{0,1,\dots,k} = 2\pi\tau_n + \pi B_{FM} f_{mod}(t_n)$.

The zero approximation, when we take into consideration the first term only of the sum in (12) $\delta(t_n, \tau_n)$, corresponds to the linear phase characteristic, which is typical for homodyne SRR. The further approximations insert nonlinearity in the function, which is the autodyne system attribute. Therefore, the main attention below in research fulfilled will be focused on revealing of ASRR signal peculiarities under conditions, when the C_{FB} parameter is commensurable with 1.

2 Numerical analysis of the autodyne response

FM ASRR signals are usually registered in the power source circuit of the UHF oscillator (the autodetection signal) or by means of oscillation amplitude variations detection. Both variations of the amplitude in the form of AAC $a_n(t_n)$ and of the autodyne current frequency in the form of AFC $\chi_n(t_n)$ give the contribution in these signal formation. To clarify the peculiarities of FM ASRR signal formation, we use the following mathematical form of the normalized modulating function $f_{mod}(t_n)$ [11] for the non-symmetrical modulation law:

$$f_{mod}(t_n) = \frac{2}{\pi} \arctan\left[\tan\left(\frac{2\pi t_n + \pi}{2}\right)\right]. \quad (13)$$

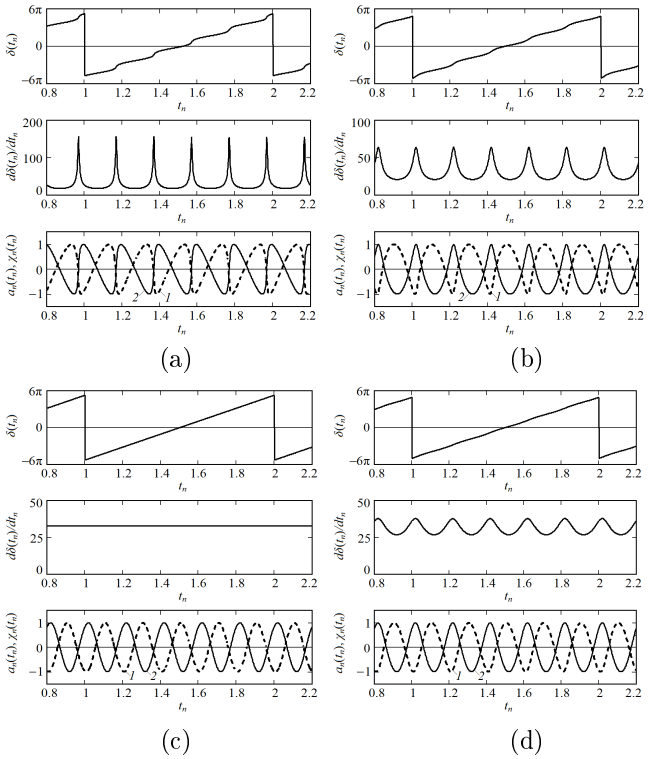

Fig. 1. Time diagrams of APC formation $\delta(t_n)$, their derivatives $d\delta(t_n)/dt_n$, AAC $a_n(t_n)$ (curve 1) and AFC $\chi_n(t_n)$ (curve 2) calculated at various values of normalized distance r_n: $r_n = 0$ (a), $r_n = 0.5$ (b), $r_n = 1$ (c) and $r_n = 1.5$ (d)

Calculation results of the time diagrams of APC $\delta(t_n)$ and its normalized derivatives $d\delta(t_n)/dt_n$ characterizing the variation speed of the reflection emission phase incursion, as well as AAC $a_n(t_n)$ and AFC $\chi_n(t_n)$, fulfilled according to (10) — (12) with account of (13) for different normalized distances r_n, are presented in Figure 1. Spectral diagrams $a_n(F_n)$ and $\chi_n(F_n)$ of signal characteristics calculated at previous values of oscillator

[2] These characteristics are determining in autodyne signal formation, therefore, they are referred as signal characteristics in the theory of autodyne systems [15].

parameters and normalized distances r_n (see Figure 1,a–d), are presented in Figure 2. In the future, at analysis on autodyne characteristics, we shall call as "operation zones" (beginning for the first, where $0 \leq r_n \leq 1$) the segments of normalized distance r_n, which are multiplies to integer numbers.

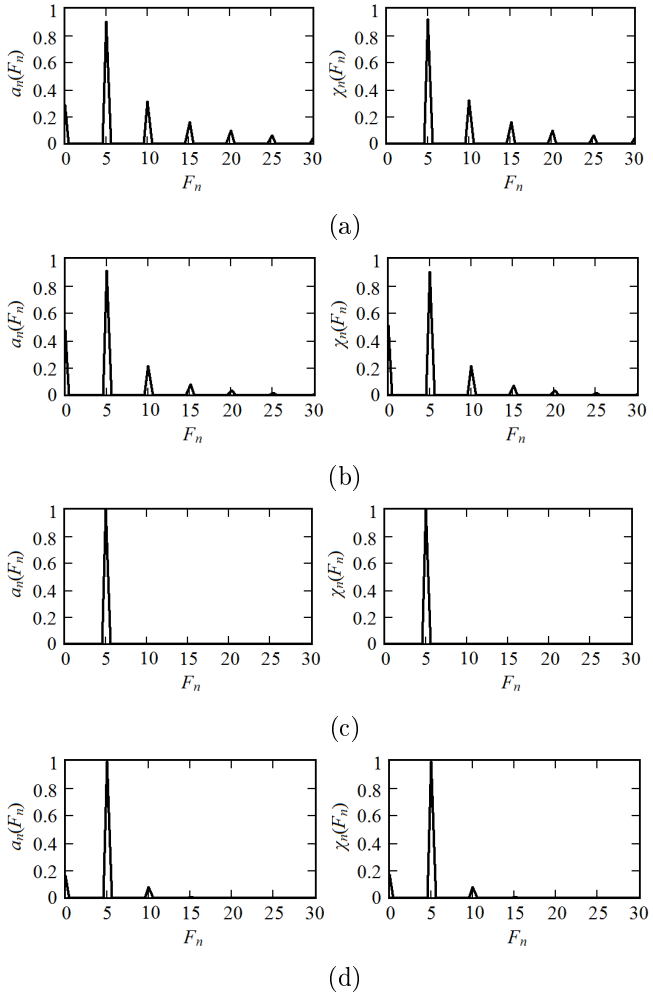

Fig. 2. Spectrograms $a_n(F_n)$ and $\chi_n(F_n)$ calculated for normalized distances $r_n = 0$ (a), $r_n = 0.5$ (b), $r_n = 1$ (c) and $r_n = 1.5$ (d)

Hereinafter, if there is not the special reservation, calculation of the time diagrams are performed at $\theta = 1$, $\psi = 0.2$, $B_{FM} = 5$, $C_{FB} = 0.8$, $k = M = 50$, $\tau_n = 0$. We note that the number of series terms in (7), (8) and approximations of k-order in (12), which were taken in calculations, ensure the convergence of calculation results in the ranges $r_n \leq 5$ and $C_{BF} \leq 0.98$.

From analysis of time and spectral diagrams presented in Figures 1,a and 2,a, we see that results obtained for $r_n = 0$ correspond to research results, which were performed in [10, 11] only for the first approximations ($\tau << T_a$). In other cases, as we see from diagrams in Figures 1,b–d and 2,b–d, with growth of the normalized distance r_n, their view essentially varies. So, for example, the APC time diagram $\delta(t_n)$ approaches to linear function, and the peak height of the normalized derivative $d\delta(t_n)/dt_n$ essentially decreases. The anharmonic distortion degree of AAC and AFC diagrams, and accordingly, the level of higher harmonic components, significantly decrease. This tendency is especially noticeable in the first operation zone, where $0 \leq r_n \leq 1$. In the case of $r_n = 1, 2, \ldots$, as well as at $C_{FB} << 1$, AFC and AAC have practically the sine view as for homodyne FM ASRR.

For more obvious representation of functions obtained, we use the generalized parameter — the total harmonic distortion (THD) factor characterizing the distortions of quasi-periodic oscillations. Calculation results of THD as a function of the normalized distance r_n, are presented in Figure 3 for different C_{FB}.

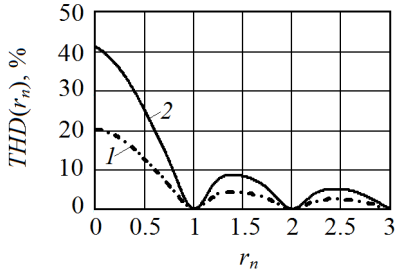

Fig. 3. Plots $THD(r_n)$ calculated for $B_{FM} = 5$ and $C_{FB} = 0.4$ (curve 1) and for $C_{FB} = 0.8$(curve 2)

From plots in Figure 3, it is seen that the most distortions of the FM ASRR signals are observed in the region of small r_n of the first operation zone. At $C_{FB} = 0.8$, THD in this zone achieves about 40%. With further transition into operation zones of higher order, signal distortions essentially decrease achieving the minimal values at the normalized distances r_n, which are multiplies of integer numbers ($r_n = 1, 2, \ldots$).

Returning to examination of calculation results presented in Figure 2, it is necessary to note a presence of DC components $a_0(F_n)$ and $\chi_0(F_n)$ in spectrograms of Figure 2a,b,d. A presence of the DC component $\chi_0(F_n)$ in the oscillator response on frequency variation $\chi_n(t_n)$ indicates to some offset of the average oscillation frequency under influence of the reflected emission. Therefore, these components deserve attention at studying FM ASRR signals. Their account may be required, for instance, at signal processing, the noise immunity analysis, etc.

Calculation results of relative levels of DS components $a_0(r_n)$ and $\chi_0(r_n)$ depending on the normalized distance r_n at $C_{FB} = 0.8$ for the autodyne responses $a_n(t_n)$ and $\chi_n(t_n)$ are presented in Figure 4.

From curves in Figure 4 we can see that in the first operation zone of the FM ASRR at large values of $C_{FB} \sim 1$ the DC component level may have values, which is commensurable with signal amplitudes. In zones with higher order, we may neglect by influence of DC components. It is necessary to note that for $C_{FB} << 1$,

DC components in the output signals of FM ASRRs are practically absent.

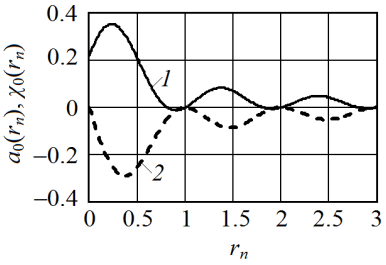

Fig. 4. Plots of $a_0(r_n)$ (curve 1) and $\chi_0(r_n)$ (curve 2) calculated for $B_{FM} = 5$ and $C_{FB} = 0.8$

To understand of the character of dependences obtained, let us introduce the concepts of equivalent feedback parameter C_{eq} of the autodyne system and the angle of dynamic displacement of phase $\Delta\delta_{DD}$ of the autodyne response: $C_{eq} = C_{FB}K_{DF}$ and $\Delta\delta_{DD} = \delta(r_n) - \delta(r_n = 0)$. Here $K_{DF} = \sum_{m=0}^{M}(-1)^m X_m(r_n)$ is the "dynamic factor" of feedback included in (8) and (12); $\delta(r_n)$, $\delta(r_n = 0)$ are phases of the instantaneous reflection factor obtained for the current value of r_n and for its zero value, relatively. Calculation results for functions $K_{DF}(r_n)$ and $\Delta\delta_{DD}(r_n)$ are presented in Figure 5, at that, for $\Delta\delta_{DD}(r_n)$ two curves are obtained: for non-isochronic (curve 1) and for isochronic (curve 2) oscillator.

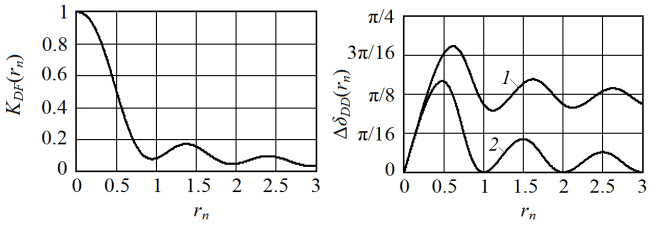

Fig. 5. Plots of the dynamic feedback factor $K_{DF}(r_n)$ (a) of FM ASRR and phase displacement $\Delta\delta_{DD}(r_n)$ (b) of signals versus the normalized distance r_n to the reflected object: $\theta = 1$ (curve 1), $\theta = 0$ (curve 2)

From the curve $K_{DF}(r_n)$ (see Figure 5a) we see that with growth of r_n in the first operation zone, where $0 < r_n < 1$, the value of K_{DF} and, hence, the equivalent parameter C_{eq} decreases practically by an order. Then, with growth of r_n, the value of C_{eq} asymptotically damps with slight growths in the middle part of the operation zones of higher order, where $r_n > 1$.

Dynamic phase variations $\Delta\delta_{DD}$ of signal characteristics, which influence on the distortion character, which is well seen from comparison of curves of Figures 1a and b, with growth of r_n in the first operation zone are also maximal. At $r_n = 1$, there is the first minimum of this value, which is determined by the θ parameter, characterizing of oscillator non-isochronous property (see Figure 5b). with further growth of r_n, the asymptotic damping of "oscillations" in dynamic phase variations $\Delta\delta_{DD}$ is here observed.

Plots of AFC $\chi_n(t_n)$ and AAC $a_n(t_n)$ are presented in Figure 6 for the case of $r_n = 2.5$ and $C_{FB} = 5$.

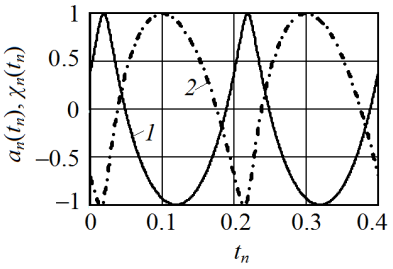

Fig. 6. Time diagrams of AFC $\chi_n(t_n)$ (curves 1) and AAC $a_n(t_n)$ (curves 2) formation calculated at $C_{FB} = 5$ and $r_n = 2.5$

As we see from plots in Figure 6, in spite of the fact that $C_{FB} > 1$, the autodyne response in higher operation zones of FM ASRR is smooth and has not jumps and breaks. At that, the distortion level of quasi-harmonic characteristics equals to 31%.

Results obtained here seem to be contradictory to the habitual representations [10, 11] and have quite explainable physical sense. For its understanding, it is enough to take the simplified model of representation of interaction process of the autodyne with the proper reflected emission, which can be described by the steps method [17]. From this model it follows that with shortening of the radio-pulse relative duration (this is equivalent to growth of normalized distance), a number of partial reflections decreases during the time period of the radio-pulse action. This leads to reduction of equivalent feedback parameter C_{eq} of the autodyne system and, hence, the signal distortion level. When r_n achieved the unity ($r_n = 1$), the reflection emission impact becomes single-partial and formation of practically harmonic autodyne variations is provided, which is shown by the above-described analysis.

3 Results of experimental investigations of FM autodynes

Experimental investigations of FM ASRR were performed with the oscillating module on 8mm-range Gunn diode in the structure of the autodyne radar developed for monitoring of point-works occupation in hump-yards [2–4]. The autodyne oscillator of this sensor was made on the base of the Gunn diode AA727A and the varicap 3A637A-6 in packaged implementation. Output power is 25 mW, the central frequency is 36.5 GHz. The UHF oscillator provides the frequency tuning of 500 MHz in the mode of linear FM. The FM law is the non-symmetric saw-tooth, the modulation frequency is 10 kHz. The antenna is horn-lens type with the pattern width 6×6 degrees.

The autodyne signal was extracted in the power source circuit of the Gunn diode with the help of the wideband current transformer. After filtering and amplification, it passes on the analog-to-digital converter of the digital signal processor (DSP) TMS320F2808 from Texas Instrument of the processor unit. In this unit, functions of modulation voltage formation, digital signal processing and communication interface RS-485 with the personal computer.

Figure 7 shows the signal spectrograms obtained from the corner reflector (a) and from the wall of five-floor building (b). The corner reflector with effective dispersion area near 10 m^2 was mounted at the distance $l = 3$ m (delay time $\tau = 2 \cdot 10^{-8}$ sec) from the ASRR antenna aperture. The building wall was situated at distance $l = 60$ m ($\tau = 4 \cdot 10^{-7}$ sec). Signal amplitudes (U_s) in both cases were practically the same. The converted signal frequency in the first case was about 100 kHz ($T_a = 1 \cdot 10^{-5}$ c), а во втором — 2 МГц ($T_a = 5 \cdot 10^{-7}$ c).

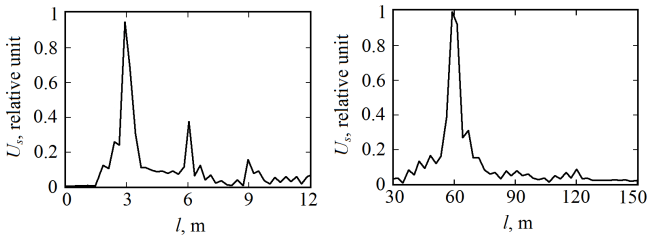

(a) (b)

Fig. 7. Spectrograms of signals converted by the autodyne obtained from the corner reflector (a) and from the wall of 5-floor building (b)

In the first case (see Figure 7a), we see in spectrograms the noticeable level of second and third harmonics typical for anharmonic distortions of the autodyne signals. In the second case, higher harmonic components are practically absent. From comparison of obtained spectrograms presented in Figures 7a,b and 2a,c, we see their qualitative agreement. Thus, obtained experimental data confirm the adequacy of above-developed mathematical model for analysis and calculation of FM ASRR signal and spectral characteristics.

Conclusions

Peculiarities of FM ASRR signal formation are considered for the non-symmetric saw-tooth law in the general case of arbitrary ratio of delay time τ of the reflected emission and the autodyne signal period T_a. At description of signal properties, the new concepts of the normalized distance r_n to reflected object, the equivalent feedback parameter C_{eq} of the autodyne system and the angle of phase dynamic displacement $\Delta\delta_{DD}$ of the autodyne response.

From analysis of the fulfilled research results the important conclusion follows that FM ASRR signal frequency in the whole range of distances to the radar object corresponds exactly to the frequency of the converted signal obtained in the case of the homodyne system [5].

In the first operation zone, at small distance to the reflected object, where the strong inequality $r_n << 1$ is true, and hence, $\tau << T_a$, the analysis results obtained are agreed with results of previous researches. In this zone, at $C_{FB} \sim 1$, significant distortions of autodyne signals and spectrum enrichment are observed, which require of its account in devices for signal processing.

With growth of normalized distance r_n, the value of equivalent feedback parameter C_{eq} of the autodyne system essentially decreases while the angle of phase dynamic displacement $\Delta\delta_{DD}$ of the autodyne response after significant variations in the first operation zone has got the steady-state value in the further zones. This approaches APC $\delta(t_n)$ to the linear function and essentially decreases the anharmonic distortion degree of AAC $a_n(t_n)$ and AFC $\chi_n(t_n)$. This feature is especially noticeable in the first operating zone if $r_n \to 1$. In the case, when r_n is the multiple of the integer number ($r_n = 1, 2, \ldots$), AAC $a_n(t_n)$ and AFC $\chi_n(t_n)$ have practically the sine view.

Signal analysis results obtained in this paper develop and expand results of known researches fulfilled in publications [15, 18] in the part of FM oscillator account as well as fulfilled in [10, 11] in the part of account (in the autodyne model) of dynamics of phase variation of reflected emission at its propagation to the object and back. Revealed regulations of signal formation in FM ASRR have rather general character, therefore, obtained results, as we think, can be used at signal calculation of autodyne systems made on the base of semiconductor laser modules [19–21].

Acknowledge

The present paper is prepared in accordance with an Agreement on scientific-technological cooperation between UrFU and IRE NASU, as well as at financial support of Russian Federation Government, order No 211, contract No 02.A03.21.0006.

References

[1] Armstrong B.M., Brown R., Rix F. and Stewart J.A. C. (1980) Use of Microstrip Impedance-Measurement Technique in the Design of a BARITT Diplex Doppler Sensor. *IEEE Transactions on Microwave Theory and Techniques*, Vol. 28, No. 12, pp. 1437-1442. DOI: 10.1109/TMTT.1980.1130263

[2] Varavin A.V., Vasiliev A.S., Ermak G.P. and Popov I.V. (2010) Autodyne Gunn-diode transceiver with internal signal detection for short-range linear FM radar sensor. *Telecommunication and Radio Engineering*, Vol. 69, No. 5, pp. 451-458. DOI: 10.1615/TelecomRadEng.v69.i5.80

[3] Ermak G.P., Popov I.V., Vasilev A.S., Varavin A.V., Noskov V.Ya. and Ignatkov K.A. (2012) Radar sensors for hump yard and rail crossing applications. *Telecommunication and Radio Engineering*, Vol. 71, No. 6, pp. 567-580. DOI: 10.1615/TelecomRadEng.v71.i6.80

[4] Noskov V.Ya., Varavin A.V., Vasiliev A.S., Ermak G.P., Zakarlyuk N.M., Ignatkov K.A. and Smolskiy S.M. (2016) Modern hybrid-integrated autodyne oscillators of microwave and millimeter wave ranges and their application. Part 9. Autodyne radar applications. *Uspekhi sovremennoi radioelektroniki*, No. 3, pp. 32-86. (in Russian).

[5] Komarov I.V. and Smolskiy S.M. (2003) *Fundamentals of short-range FM radar*. Norwood: Artech House, 289 p.

[6] Hinman W.S. and Brunetti C. (1946) Radio Proximity-Fuze Development. *Proceedings of the IRE*, Vol. 34, No. 12, pp. 976-986. DOI: 10.1109/JRPROC.1946.233235

[7] Takayama Y. (1973) Doppler signal detection with negative resistance diode oscillators. *IEEE Transactions on Microwave Theory and Techniques*, Vol. 21, No. 2, pp. 89-94. DOI: 10.1109/TMTT.1973.1127929

[8] Jefford P.A. and Howes M.S. (1985) Modulation schemes in low-cost microwave field sensor. *IEEE Transaction of Microwave Theory and Technique*, Vol. 31, No. 8, pp. 613-624. DOI: 10.1109/TMTT.1983.1131559

[9] Votoropin S.D. and Noskov V.Ya. (2002) Analysis of operating regimes of EHF hybrid-integrated autodynes based on the Gunn micro power mesa planar diodes. *Russian Physics Journal*, Vol. 45, No. 2, pp. 195-206. DOI : 10.1023/A:1019664300993.

[10] Votoropin S.D., Noskov V.Ya. and Smolskiy S.M. (2008) An analysis of the autodyne effect of oscillators with linear frequency modulation. *Russian Physics Journal*, Vol. 51, No. 6, pp. 610-618. DOI: 10.1007/s11182-008-9083-5

[11] Votoropin S.D., Noskov V.Ya. and Smolskiy S.M. (2009) Modern Hybrid-Integrated Autodyne Oscillators of Microwave and Millimeter Range and Their Applications. Research of Autodynes with Frequency Modulation. *Uspehi sovremennoi radioelektroniki*, no. 3, pp. 3-50. (in Russian).

[12] Noskov V.Ya., Vasiliev A.V., Ermak G.P., Ignatkov K.A. and Chupahin A.P. (2016) Mathematical model of FM autodyne radar. *Physics and Engineering of Microwaves, Millimeter and Submillimeter Waves (MSMW), 2016 9th International Kharkiv Symposium on*, A-25, pp. 1-4. DOI: 10.1109/MSMW.2016.7538101

[13] Noskov V.Ya., Vasiliev A.V., Ermak G.P., Ignatkov K.A. and Chupahin A.P. (2016) Main expressions for analysis of signals and noise of autodyne FM radar. *Physics and Engineering of Microwaves, Millimeter and Submillimeter Waves (MSMW), 2016 9th International Kharkiv Symposium on*, A-9, pp. 1-4. DOI: 10.1109/MSMW.2016.7538019

[14] Ignatkov K.A. and Vasiliev A.V. (2016) Signals of the autodyne FM radar for mm-wavelength range. *Microwave & Telecommunication Technology (CriMiCo), 2016 26-th International Crimean Conference*, Vol. 10, pp. 2139-2145.

[15] Noskov V.Ya. and Ignatkov K.A. (2013) Autodyne signals in case of random delay time of the reflected radiation. *Telecommunication and Radio Engineering*, Vol. 72, no. 16, pp. 1521-1536. DOI: 10.1615/TelecomRadEng.v72.i16.70

[16] Noskov V.Ya. and Ignatkov K.A. (2014) About applicability of quasi-static method of autodyne systems analysis. *Radioelectronics and Communications Systems*, Vol. 57, No. 3, pp. 139-148. DOI: 10.3103/S0735272714030054.

[17] Noskov V.Ya. and Ignatkov K.A. (2013) Dynamics of autodyne response formation in microwave generators. *Radioelectronics and Communications Systems*, Vol. 56, No. 5, pp. 227-242. DOI: 10.3103/S0735272713050026

[18] Noskov V.Ya. and Ignatkov K.A. (2013) Dynamic features of autodyne signals. *Russian Physics Journal*, Vol. 56, No. 4, pp. 420-428. DOI: 10.1007/s11182-013-0051-3

[19] Giuliani G, Norgia M, Donati S. and Bosch T. (2002) Laser diode self-mixing technique for sensing applications. *Journal of Optics A: Pure and Applied Optics*, Vol. 4, No. 6, pp. 283-294. DOI: 10.1088/1464-4258/4/6/371

[20] Sobolev V.S. and Kashcheeva G.A. (2008) Self-mixing frequency-modulated laser interferometry. *Optoelectronics, Instrumentation and Data Processing*, Vol. 44, No. 6, pp. 519-529. DOI: 10.3103/S8756699008060058

[21] Usanov D.A., Skripal A.V. and Astakhov E.I. (2014) Determination of nanovibration amplitudes using frequency-modulated semiconductor laser autodyne. *Quantum Electronics*, Vol. 44, No. 2, pp. 184-188. DOI: 10.1070/QE2014v044n02ABEH015176

Особливості формування сигналів автодинних радіолокаторів із лінійною частотною модуляцією

Носков В. Я., Ігнатков К. А., Чупахін А. П., Васильєв А. С., Єрмак Г. П., Смольський С. М.

Представлені результати досліджень особливостей формування сигналів автодинних систем ближньої радіолокації міліметрового діапазону з лінійною частотною модуляцією по несиметричному пилкоподібному закону. Отримані вирази для розрахунку автодинних сигналів в загальному випадку довільного часу запізнювання відбитого випромінювання. Побудовано тимчасові і спектральні діаграми автодинних сигналів для випадків, коли тривалість їх періоду значно більше часу запізнювання відбитого випромінювання, а також для випадків, коли така нерівність не виконується. Експериментальні дослідження виконані із застосуванням генератора на діоді Ганна 8-мм діапазону довжини хвиль, електрично керованого по частоті варикапом.

Ключові слова: автодін; автодинний сигнал; автодинний відгук; система ближньої радіолокації; частотна модуляція; генератор на діоді Ганна

Особенности формирования сигналов автодинных радиолокаторов с линейной частотной модуляцией

Носков В. Я., Игнатков К. А., Чупахин А. П., Васильев А. С., Ермак Г. П., Смольский С. М.

Представлены результаты исследований особенностей формирования сигналов автодинных систем ближней радиолокации с линейной частотной модуляцией по несимметричному пилообразному закону. Получены выражения для расчёта автодинных сигналов в общем случае произвольного времени запаздывания отражённого излучения. Построены временные и спектральные диаграммы автодинных сигналов для случаев, когда продолжительность их периода значительно больше времени запаздывания отражённого излучения, а также для случаев, когда данное неравенство не выполняется. Экспериментальные исследования выполнены с применением генератора на диоде Ганна 8-мм диапазона длин волн, электрически управляемого по частоте варикапом.

Ключевые слова: автодин; автодинный сигнал; автодинный отклик; система ближней радиолокации; частотная модуляция; генератор на диоде Ганна